processes

MDPI

Article

Helium Geochemical Characteristics and Favorable Zones in the Tarim Basin: Implications for Helium Exploration

Haijun Yang [1,2,3], Pengpeng Li [4,5,*], Haizu Zhang [1,2,3], Jiahao Lv [6,7], Wen Zhang [1,2,3], Jiarun Liu [4], Shaoying Huang [1,2,3], Xianzhang Yang [1,2,3], Wenfang Yuan [1,2,3] and Xiang Wang [1,2,3]

1 R&D Center for Ultra-Deep Complex Reservoir Exploration and Development, China National Petroleum Corporation (CNPC), Korla 841000, China; yanghaij-tlm@petrochina.com.cn (H.Y.); zhanghz-tlm@petrochina.com.cn (H.Z.); zhwen-tlm@petrochina.com.cn (W.Z.); huangsy-tlm@petrochina.com.cn (S.H.); yangxz-tlm@petrochina.com.cn (X.Y.); yuanwf-tlm@petrochina.com.cn (W.Y.); wxiang-tlm@petrochina.com.cn (X.W.)
2 Engineering Research Center for Ultra-Deep Complex Reservoir Exploration and Development, Xinjiang Uygur Autonomous Region, Korla 841000, China
3 Research Institute of Petroleum Exploration and Development, Tarim Oilfield Company, PetroChina, Korla 841000, China
4 Institute of Energy, Peking University, Beijing 100871, China; 2201110689@stu.pku.edu.cn
5 Key Laboratory of Petroleum Resources Research, Gansu Province, Northwest Institute of Eco-Environment and Resources, Chinese Academy of Sciences, Lanzhou 730000, China
6 State Key Laboratory of Lithospheric Evolution, Institute of Geology and Geophysics, Chinese Academy of Sciences, Beijing 100029, China; lvjiahao222@mails.ucas.ac.cn
7 University of Chinese Academy of Sciences, Beijing 100049, China
* Correspondence: lipengpeng@pku.edu.cn

Abstract: Helium is an irreplaceable ore resource for many applications, such as nuclear magnetic resonance, aviation, semiconductors, and nuclear energy. Extracting helium in a free state from natural gas is currently the only economical approach at the industrial level. In this study, we compiled geochemical data of 719 natural gas samples from 36 oil and gas fields in the Tarim basin that include experimental results and previously reported data. Helium is of primarily crustal origin in the Tarim Basin according to helium isotope characteristics (not exceeding 0.1 Ra), except in the Ake gas field that has not more than 7% of mantle helium. Helium concentrations in diverse tectonic units vary considerably. Oil-type gas, on the whole, has a higher helium concentration relative to coal-type gas. Abundant helium flux, a favorable fault system between the source-reservoir system, no strong charging of gaseous hydrocarbons, and the good sealing capacity are important factors that control the formation of helium-rich gas fields. Considering both the helium concentration and natural gas reserves, helium-rich gas fields located in the Southwest Depression and Tabei Uplift can be regarded as the major favorable zones of further deployment for helium extraction.

Keywords: Tarim Basin; helium; natural gas; geochemical characteristics; favorable zones

Citation: Yang, H.; Li, P.; Zhang, H.; Lv, J.; Zhang, W.; Liu, J.; Huang, S.; Yang, X.; Yuan, W.; Wang, X. Helium Geochemical Characteristics and Favorable Zones in the Tarim Basin: Implications for Helium Exploration. *Processes* **2024**, *12*, 1469. https://doi.org/10.3390/pr12071469

Academic Editor: Carlos Sierra Fernández

Received: 3 June 2024
Revised: 6 July 2024
Accepted: 8 July 2024
Published: 13 July 2024

1. Introduction

Due to its unique physical and chemical properties, Helium (He) plays a central role in many high-tech manufacturing applications such as magnetic resonance imaging, superconductivity, welding, cryogenics, leak detection, controlled atmospheres, pressurization and purging, heat transfer, laboratory analysis, lift gas, airships, and weather balloons [1–3]. Helium resources are distributed extremely unevenly around the globe. The United States accounts for 35% of the global helium resources (484×10^8 m^3, as of the end of 2021), followed by Qatar (21%), Algeria (17%), Russia (14%), Canada (4%), and China (2%) [4]. Moreover, major helium-producing countries have enacted laws to protect helium resources due to persistent supply–demand imbalances in the global helium market. China imports

nearly all of its helium, with its external dependency exceeding 95%. Such conditions seriously threaten national helium security. Therefore, it is imperative to objectively analyze the current helium distributions in China, as a basis for achieving an increasingly independent helium supply in the future.

There are four technologies for helium extraction, namely, extraction from natural gas, exhaust during ammonia synthesis, air, and uranium ore [5]. Extracting helium in a free state from natural gas or the residues of liquefied natural gas is currently the only economical method at the industrial level [6–8]. This is mainly because (1) helium concentration in natural gas is higher after continuous enrichment over a geological timescale, (2) this technology has the lower process costs and higher effectiveness, and (3) natural gas itself is an extremely important fuel. Performing helium exploration, particularly specializing in the enrichment zones of natural gas (mainly CH_4 in this study), is therefore a significant aspect of the discovery of gas fields with abundant helium resources.

At the beginning of the 20th century, natural gas fields with helium concentrations above 0.3% in the USA were required to extract helium within natural gas using a cryogenic process [9]. At present, in most commercial helium-rich gas fields (He > 0.1%), helium extraction is carried out using advanced extracting technology due to increasing global demand. Examples of these gas fields include the Weiyuan, Hetianhe, and Dongsheng gas fields in China, the Hugoton-Panhandle gas field in the USA, and the Hassi R'Mel gas field in Algeria. Although the North Pars gas field in Qatar has a helium concentration of only 0.04%, far less than the commercial threshold for helium extraction, it is a large-scale commercial field for helium supply around the globe. Due to the need for large-scale natural gas exports, natural gas in this gas field must undergo a series of liquefaction processes, thus causing the substantial increase in helium concentration in the residues of liquefied natural gas. Using the LNG-BOX technology to extract helium from the residues of liquefied natural gas has increased helium production in Qatar significantly. In recent years, annual helium production in Qatar has been up to tens of millions of cubic meters, ranking second globally, only after the USA. To sum up, at the current industrial extraction level, the economic threshold for extracting helium from natural gas is approximately 0.05%. Once above 0.1%, extracting helium from natural gas is especially worthwhile. If below 0.05%, natural gas is much less economical for helium extraction.

The Tarim Basin has very abundant natural gas resources and is one of very important natural gas production bases in China [10–14], producing more than 350×10^8 m^3 of natural gas in 2022. Preliminary statistics concerning the helium concentrations of natural gas samples have shown that some gas fields, which are tectonically located in the Tabei Uplift, North Depression, Tazhong uplifts, and Southwest Depression in the Tarim Basin, have helium concentrations above commercial threshold [5,15]. Therefore, the Tarim Basin has abundant helium resources. However, the study of factors affecting the distributions of helium resources is still in its infancy.

To date, with the sole exception of a case discovered in 2017 in the Tanzanian section of the East African Rift, almost all commercial/valuable helium systematics have been discovered as a purely serendipitous by-product of petroleum exploration [16]. This is due to the fact that (1) very few exploration campaigns in the past century have specifically targeted a helium systematic, and (2) helium geochemical abnormalities, especially helium isotopes, are used to trace the interactions between diverse circles of the Earth [8]. Although many hydrothermal vents and spring seeps have occurred high helium concentrations [17–21], extracting helium in a water-soluble state from helium-rich fluids is extremely challenging, possibly due to limited daily helium production.

According to helium isotope characteristics, knowledge of helium origins in Chinese petroliferous basins has been well demonstrated. Helium in central and western cratonic basins has shown almost a completely crustal origin, but in eastern tectonically active zones has a crust–mantle complex origin [6,7,22–27]. However, the mechanism of determining helium accumulation in sedimentary basins is still its infancy, which restricts the further deployment of exploration for helium resources. In this work, we compiled 719 natural

gas samples from production wells in 36 oil and gas fields in the Tarim Basin, China (see Table S1), for further insight into helium systematics. The first objective was to demonstrate the major factors affecting helium accumulation based on the anatomy of typical gas fields. The other was to map the distributions of helium concentrations throughout this basin, optimizing favorable zones for further helium exploration.

2. Geological Setting

The Tarim Basin is the largest inland basin in China, with an area of approximately 560,000 km^2 [28]. The basin is bounded by Tianshan Mountain to the north and Kunlun Mountain and Altun Mountain to the south [28]. The Tarim Basin has Sinian-Paleozoic marine strata, Mesozoic transitional strata, and Cenozoic terrestrial strata from bottom to top, with a maximum thickness of 17~18 km. These strata overlie the metamorphic pre-Proterozoic basement rocks [13]. The Tarim Basin underwent multiple episodes of tectonic movements, creating the complicated tectonic framework of "three uplifts and four depressions", namely, Tabei Uplift, Central Uplift, Southeast Uplift, Kuqa Depression, North Depression, Southwest Depression, and Southeast Depression [13,28].

Ultra-thick sedimentary rocks in this basin can be divided into three sections on the basis of the depositional characteristics, as well as tectonic and thermal evolution histories, namely, Sinian-Lower Paleozoic, Upper Paleozoic, and Mesozoic-Cenozoic tectonic systems [29]. The Sinian-Lower Paleozoic tectonic system is predominately comprised of marine carbonate rocks except for a portion of marine clastic sediments in the Silurian and Middle-Upper Ordovician sections. In this tectonic system, multiple sets of marine source rocks mainly developed in the Northern Depression as well as its periphery, and the Markit Slope, such as the Cambrian Yuertusi, Xishanbulake, and Xidashan formations, as well as the Ordovician Yingshan and Lianglitage formations. This process was strongly associated with the development of the Nanhua Period-Sinian aulacogen [13,28]. These source rocks were matured to over-matured stages [13], producing extremely abundant hydrocarbon fluxes, resulting in the formation of many different types of oil and gas fields in the platform area of this basin, specifically of the Tabei Uplift, Northern Depression, Southeast Uplift, and Central Uplift [28]. Examples of these fields include dry gas (Kela2, Dabei), wet gas (Yingnan), condensate gas (Shunbei, Yaha, Tazhong), normal oil (Halahatang, Donghe, Hade), and heavy oil (Tahe). The Upper Paleozoic tectonic system is mainly composed of clastic rocks; only the Carboniferous section mostly consists of carbonate rocks with locally developed gypsum [13]. During this tectonic system, Carboniferous-Permian marine source rocks that were mainly developed in southwest area of this basin were matured to highly matured stages [29]. This set of source rocks was the primary source of the Permian, Jurassic, and Cretaceous oil and gas fields in the southwest area of this basin [28]. The Mesozoic-Cenozoic tectonic system primarily consists of terrestrial clastic rocks throughout the Tarim Basin, except for locally developed Paleogene marine carbonate rocks in the Southwest Depression. Multiple sets of terrestrial source rocks, such as mudstone, carbonaceous shale, and coal, mainly developed in the Kuqa Depression [13,28].

3. Material and Methods

A comprehensive dataset of 719 natural gas samples for 36 oil or gas fields in the Tarim Basin was compiled using both the geochemical data reported by previous studies (N = 297) [10,13,14,30–40] and the experimental results in this study (N = 422). An outline of the procedures of samplings and experiments is as follows. Almost all samples were collected directly from active wellheads using a high-pressure steel cylinder equipped with two valves on each end. Before sampling, the steel cylinder was flushed using active wellhead gases for up to 20 min to remove air. The pressure of natural gases inside the cylinder reached several to dozens of times higher than that of the atmosphere. The two ends of cylinder were inserted into salt-saturated water to detect leakage. Subsequently, helium concentrations and isotopes for most samples were determined using a noble gas

isotope mass spectrometer. The researchers followed the detailed procedures and test conditions of previous studies.

In this work, except for the minority of samples from exploration wells that were collected using a high-pressure steel cylinder, the majority of samples used in the present study were collected using an air trap that connected to the producing well heads. Before sampling, all air traps were vacuumized to avoid air contamination. The chemical compositions of all natural gas samples were determined using an Agilent 6890 Gas Chromatograph (Agilent Technology Co. Ltd., Santa Clara, CA, USA), equipped with a DC + PORAPAK + 13X column and a thermal conductivity detector (250 °C) in the Tarim Oilfield Company, using nitrogen as the carrier gas. The column was set to 30 °C.

Detection of low helium concentration via a gas chromatograph frequently shows greater uncertainty, especially below 50~100 ppm. Comparisons of the helium concentration results of 13 natural gas samples from three large gas fields (DB, KL2, and KS gas fields) in the Kuqa Depression, where natural gases has average helium concentrations of approximately 50 ppm, were carried out using a gas chromatograph and a noble gas isotope mass spectrometer, respectively. The relative error of each sample selected was very small, below 0.1%, except for DB302 (1.61%) and KS206 (3.56%), as shown in Figure 1. This indicates that the helium concentration results determined in this study using an Agilent 6890 Gas Chromatograph are highly reliable.

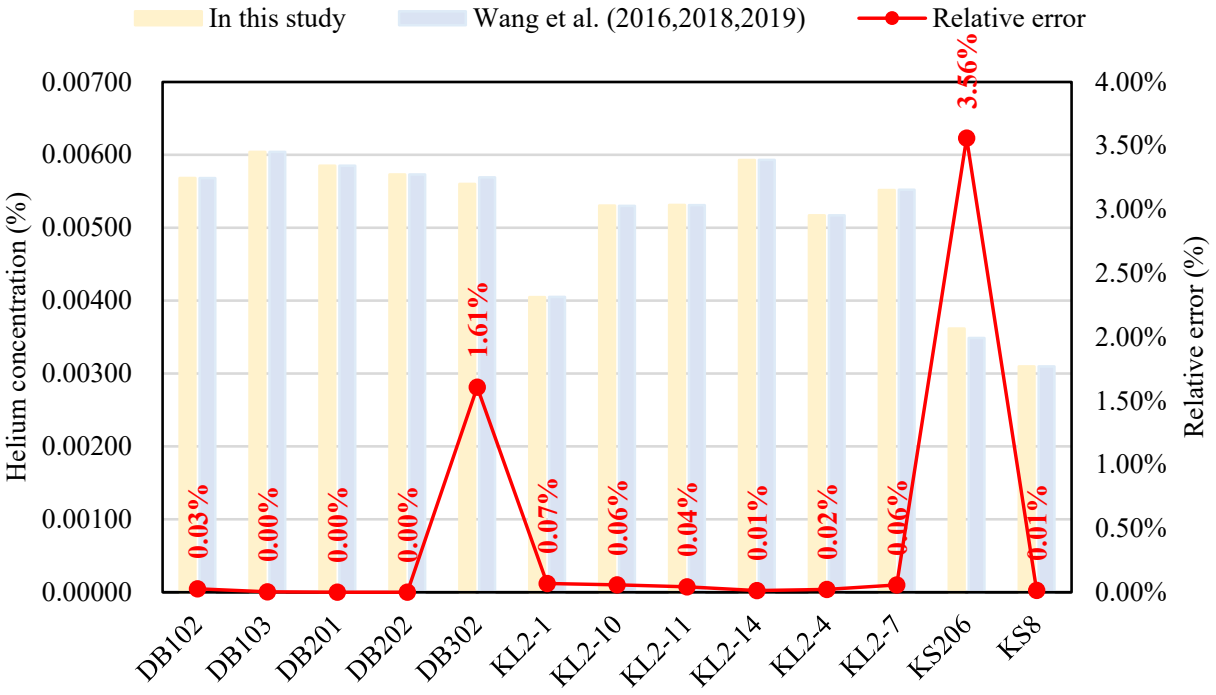

Figure 1. Comparisons of relative errors concerning the helium concentration of 13 natural gas samples obtained using a gas chromatograph and a noble gas isotope mass spectrometer, respectively [36–38].

4. Results

4.1. Distributions of Helium Concentrations in the Tarim Basin

4.1.1. Helium Concentrations in Different Gas Fields

Helium concentrations for 36 oil and gas fields in the Tarim Basin are shown in Figure 2. Seven gas fields, namely, YML, YKL, LN, HTH, YSD, BSTP, and AK, and one oil field (HD) have helium concentrations above 0.1%. Eight oil and gas fields, namely, YTK, DHT, TZ, KKY, SB, JFQ, HQQ, and DWQ, have helium concentrations of 0.05~0.1%. The other 21 oil and gas fields have helium concentrations below the commercial threshold, indicating that helium extraction would not be economical in these regions using current technology. From

the perspective of the tectonic unit, these oil and gas fields with helium concentrations above 0.05% are mainly concentrated in the Tabei Uplift and Southwest Depression.

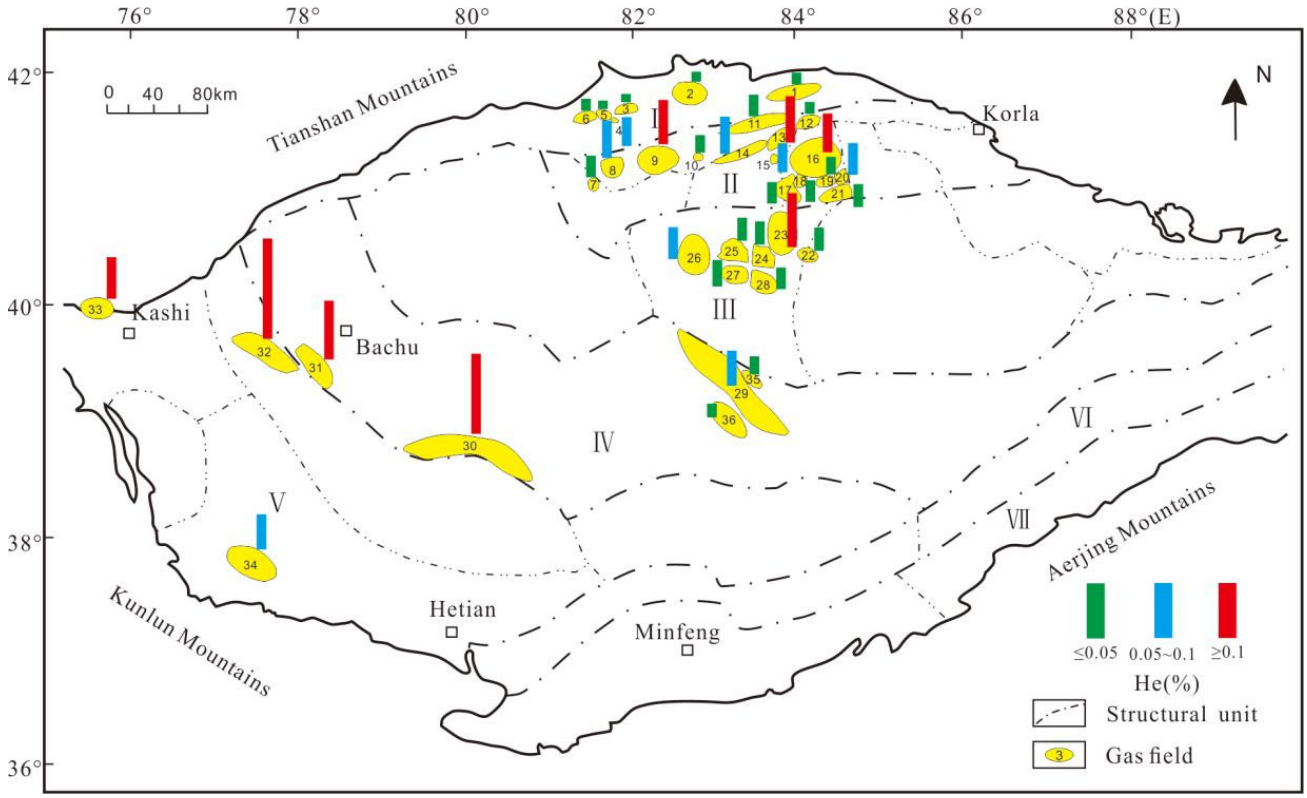

Figure 2. Helium concentrations for 36 oil and gas fields in the Tarim Basin. STM, QG, DLB, and YSD only have a helium concentration result, and the other 32 oil and gas fields have average helium concentrations. Almost all oil and gas fields that have helium concentrations above 0.05% (commercial extraction threshold) are concentrated in the Tabei Uplift and Southwest Depression. In addition to KKY, the other four gas fields in the Southwest Depression, namely, AK, HTH, BSTP, and YSD, have helium concentrations of more than 0.1%. I: Kuqa Depression, II: Tabei Uplift, III: North Depression, IV: Central Uplift, V: Southwest Depression, VI: Southeast Uplift, VII: Southeast Depression. 1: DN, 2: KL2, 3: KS, 4: DWQ, 5: DB, 6: BZ, 7: YD, 8: YTK, 9: YML, 10: HQQ, 11: YH, 12: DLB, 13: YKL, 14: DHT, 15: QG, 16: LN, 17: TH, 18: LG, 19: STM, 20: JFQ, 21: JLK, 22: YK, 23: HD, 24: FY, 25: YM, 26: SB, 27: GL, 28: MS, 29: TZ, 30: HTH, 31: YSD, 32: BSTP, 33: AK, 34: KKY, 35: ZH, 36: ZG.

4.1.2. Helium Concentration at Diverse Depths

Variations in helium concentrations along with buried depth (over 8000 m) are shown in Figure 3. With the increase in depth, the envelope line of helium concentrations presents a downward trend before 4500 m below the surface, but a dramatic increase and then a quick decrease with almost the same gradients between 4500 m and 6500 m below the surface. Afterward, a continuous decrease close to a trace amount with a significantly small slope after 6500 m below the surface can be observed. The Envelope line of helium concentrations does not follow an increasingly upward trend as the depth decreases, which indicates that there may be multiple factors affecting helium accumulation for diverse oil and gas fields in the Tarim Basin, not only dissolution/ex-dissolution.

At a depth of between 4500 m and 6500 m, the locations with dramatically elevated helium concentrations mainly include the YML gas field and HD oil field. These high helium concentrations are closely related to the magma intrusion due to the Early Permian Tarim Large Igneous Province. Evidence from seismic data, drilling campaigns, and lithogeochemistry all supports the presence of magma intrusion in these two fields [41,42].

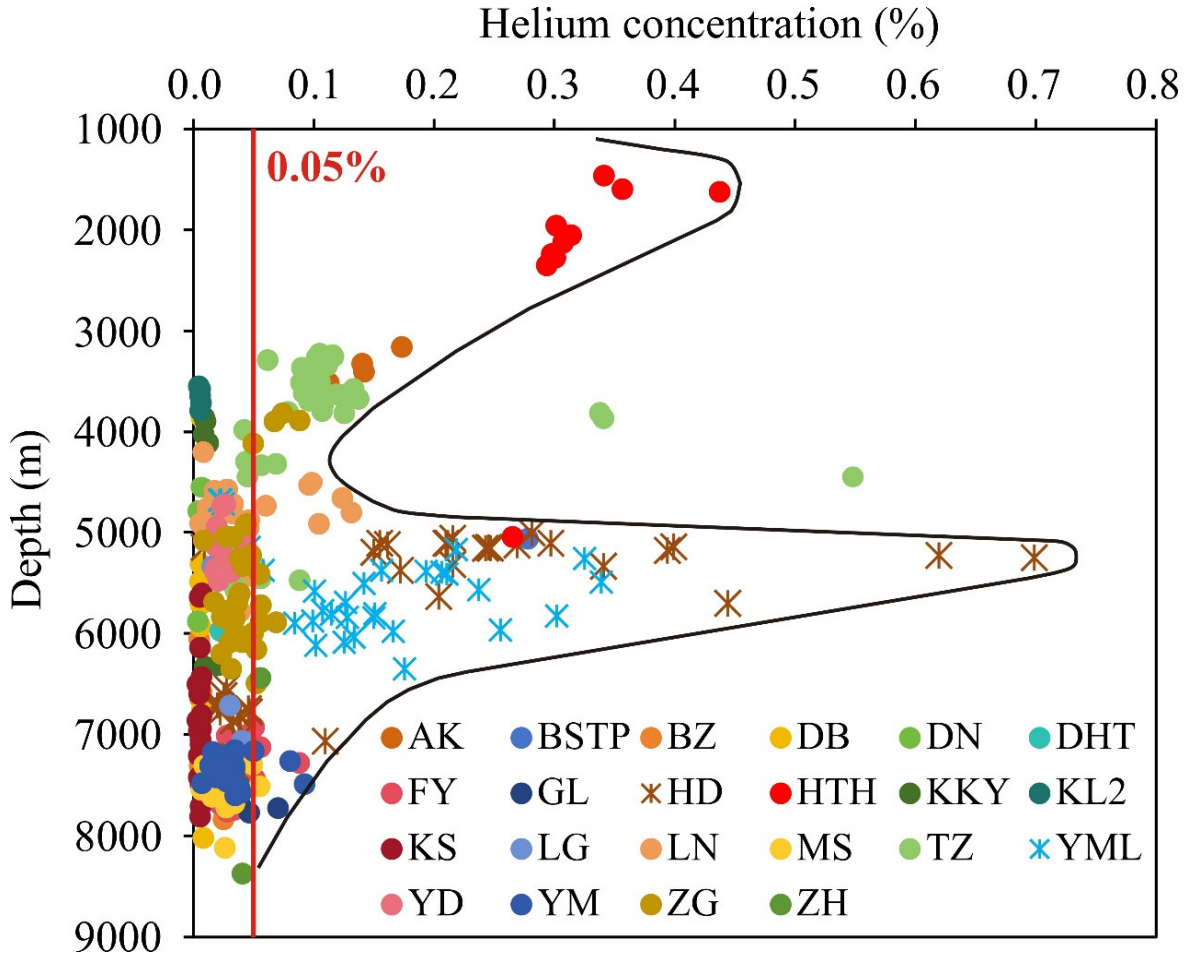

Figure 3. Helium concentrations at diverse depths in the Tarim Basin.

4.1.3. Helium Concentrations in Reservoirs with Different Geological Ages

Multiple reservoirs in the Tarim Basin from the Cambrian period to the Neogene period include helium concentrations with very great differences (Figure 4). As is well known, helium flux is a function of the decay time of radioactive elements. However, helium concentrations in the Tarim Basin do not seriously follow the rule that the older the reservoir is, the higher the helium concentrations are, indicating the complexity of helium accumulation. Despite this, on the whole, helium concentrations in the Paleozoic strata are the highest, followed by the Mesozoic and the Cenozoic strata.

In certain production layers with the same geological age, different oil and gas fields have varying levels of helium. The Ordovician stratum is one of important production layers for many oil and gas fields, such as the LG, LN, YML, YKL, ZG, FY, MS, GL, SB, YK, YM, TZ, and HTH fields. Among them, only the HTH, YML, YKL fields have helium concentrations commonly above 0.1%. The Cretaceous strata are another primary production layers for some oil and gas fields, such as the AK, YKL, YML, KS, KL2, DB, and BZ fields. Only the YML and AK field have helium concentrations commonly above 0.1%, and the YKL field is close to the economic threshold (0.05%).

In certain gas fields that have multiple production layers, helium concentrations in different production layers may also vary greatly. The YKL gas field includes at least four production layers, namely, the Cambrian, Ordovician, Cretaceous, and Paleogene reservoirs from bottom to top. Helium concentrations in these four sets of reservoirs are from 0.03% to 0.34% (0.11% on average), from 0.07% to 0.94% (0.22% on average), from far below 0.01% to 0.19% (0.04% on average), and from far below 0.01% to 0.07% (0.03% on average), respectively. In the YKL gas field, the Cambrian and Ordovician reservoirs close

to the basement have a greater helium concentration, but the Cretaceous and Paleogene reservoirs far away from the basement have helium concentrations below 0.05%.

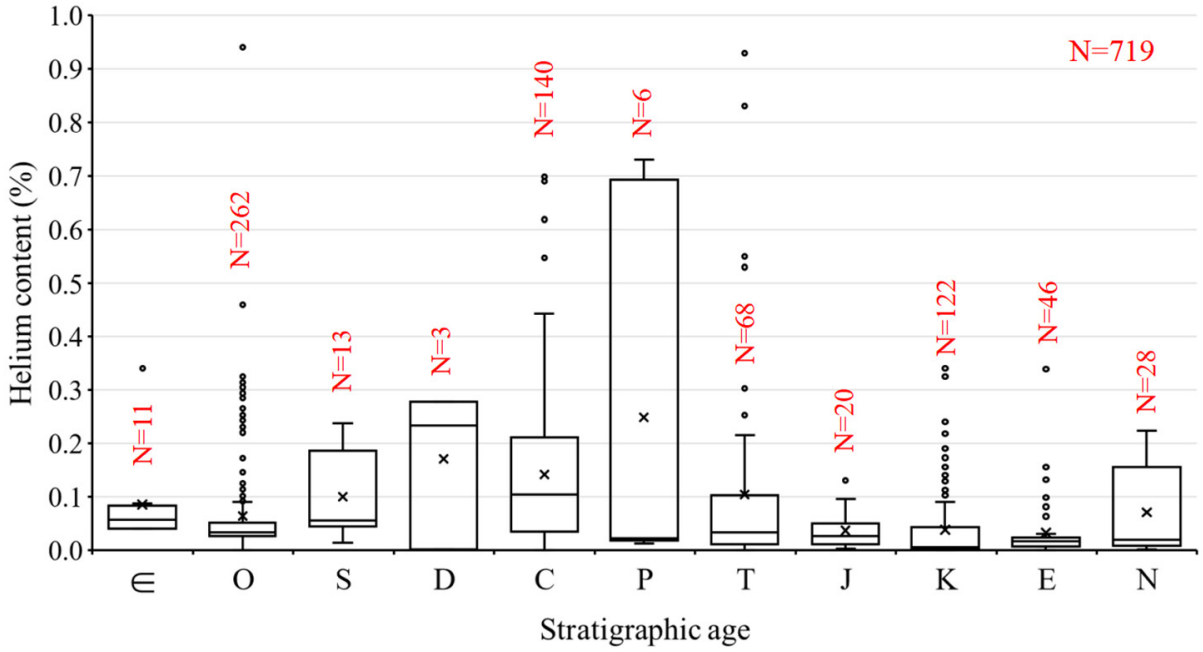

Figure 4. Box plot showing helium concentrations in diverse strata with different geological ages in the Tarim Basin.

4.1.4. Helium Concentration in Diverse Types of Natural Gases

In the Tarim Basin, there are mainly two types of natural gases, coal-type and oil-type gases. They can be roughly distinguished according to the $\delta^{13}C$ of both C_2H_6 and C_3H_8 [43]. Oil-type gas is concentrated in all Paleozoic and some Mesozoic strata of the platform area of this basin, such as the Tabei Uplift, Northern Depression, Southeast Uplift, and Central Uplift, whereas coal-type gas is largely localized in the Cenozoic strata of the Kuqa Depression [13,33].

As shown in Figure 5, diverse helium concentrations occurring in both coal-type and oil-type gases could be found. However, almost all samples with helium concentrations above 0.1% fall within the zone of oil-type gas ($\delta^{13}C_2H_6 < -28‰$ and $\delta^{13}C_3H_8 < -25‰$), except for some samples from the YKL gas fields and all samples from the YML gas field located in the zone of coal-type gas ($\delta^{13}C_2H_6 > -28‰$ and $\delta^{13}C_3H_8 > -25‰$). Samples with helium concentrations between 0.05% and 0.1% fall within the zones of either coal-type or oil-type gas, among which over seventy percent of samples are located in the zone of oil-type gas. All samples with helium concentrations below 0.05% fall within the zone of coal-type gas.

Oil-type gas primarily originates from the Cambrian-Ordovician marine source rocks, whereas coal-type gas is predominantly sourced from the Triassic-Jurassic terrestrial source rocks [13,28]. Oil-type gas is prone to capturing the abundant helium flux from the massive basement granite-metamorphic rocks relative to coal-type gas. In addition, the Cambrian-Ordovician marine source rocks have higher concentrations of radioactive elements, such as U and Th, relative to the Triassic-Jurassic terrestrial source rocks, and the former had a longer time to produce helium. As a result, these conditions favor helium accumulation in oil-type gas. However, anomalously high helium concentrations (above economic threshold, 0.05%) in some coal-type gas field, such as the HQQ, YML, KKY, YTK, and AK gas fields, are due to the direct connection between the source and reservoir systems through developed deep-seated fractures that cause the upward migration of abundant helium flux into overlying reservoirs.

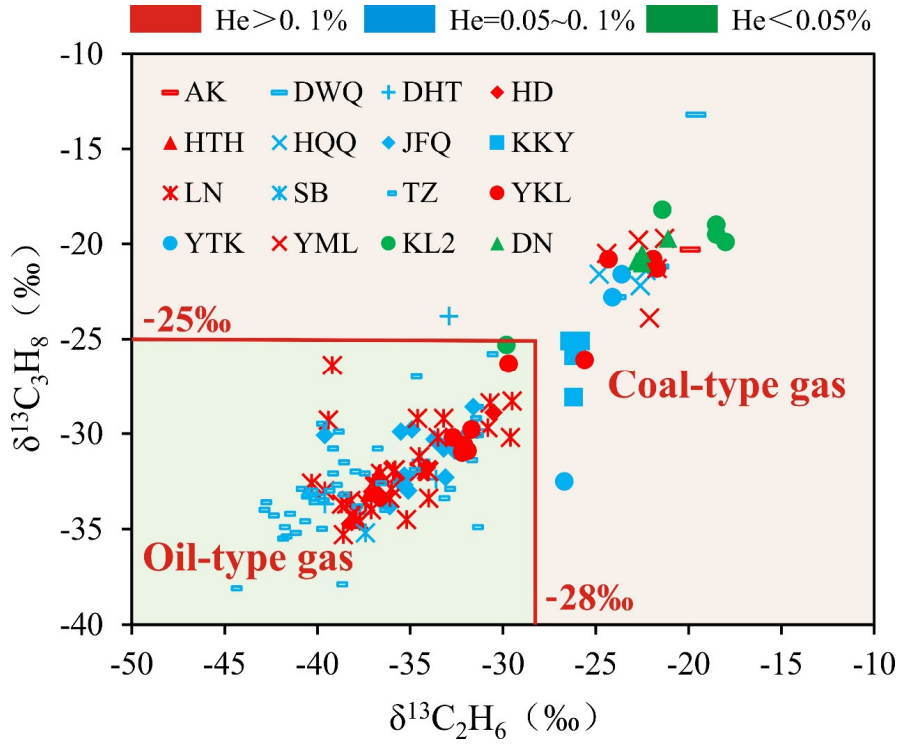

Figure 5. Helium concentrations in coal-type and oil-type gases. Coal-type and oil-type gases are roughly distinguished according to the $\delta^{13}C$ of both C_2H_6 and C_3H_8 [43] (coal-type gas: $\delta^{13}C_2H_6 > -28‰$ and $\delta^{13}C_3H_8 > -25‰$, oil-type gas: $\delta^{13}C_2H_6 < -28‰$ and $\delta^{13}C_3H_8 < -25‰$).

4.2. Helium Isotopes in the Tarim Basin

It has been demonstrated that helium isotopes (R/Ra), where R is the $^3He/^4He$ ratio of samples and Ra is the atmospheric $^3He/^4He$ ratio (1.4×10^{-6}), represent an ideal proxy to trace helium origin in oil and gas fields [7,26,44–47]. A widely accepted assumption is that helium isotopes can be simply regarded as the mixing of mantle-derived and crust-derived helium. Typical values for mantle-derived and crust-derived end-members are 0.02 Ra and 8 Ra, respectively [6,24,48–50]. As a result, the contribution of mantle-derived helium, therefore, can be evaluated quantitatively using a crust-mantle two-endmembers mixing model [47]. Generally, the higher R/Ra value, the greater the contribution of mantle-derived helium to natural gas. The R/Ra value of below 0.1% indicates that helium is predominantly sourced from a radioactive origin, without contamination from the mantle origin [23].

R/Ra values for different oil and gas fields in the Tarim Basin are shown in Figure 6. Helium isotopes of all samples range from 0.02 Ra to 0.60 Ra. The vast majority of samples are below 0.1 Ra, indicating that most oil and gas fields in the Tarim Basin only include crust-derived helium. A minority of samples from DHT, YH, JFQ, JLK, and YKL gas fields in the Tabei Uplift have R/Ra values between 0.1 and 0.2 [13,14], which is associated with either the presence of lithium-rich intrusive igneous rocks [13] or the primordial ^3He enclosed in the inclusions and the matrix of intrusive igneous rocks. On the other hand, all samples from the AK gas field in the western margin of the Southwest Depression have helium isotope between 0.55 Ra and 0.60 Ra [14], indicating that mantle-derived helium contributes at most 7% to this gas field. This is closely related to mantle degassing via deep-rooted faults developed due to intense compression between the Pamirs and the South Tianshan Mountain. To sum up, such helium isotope characteristics in the Tarim Basin indicate that this basin is overwhelmingly dominated by crust-derived helium, with little significant mantle-derived helium, except for the area close to the western margin of the Southwest Depression.

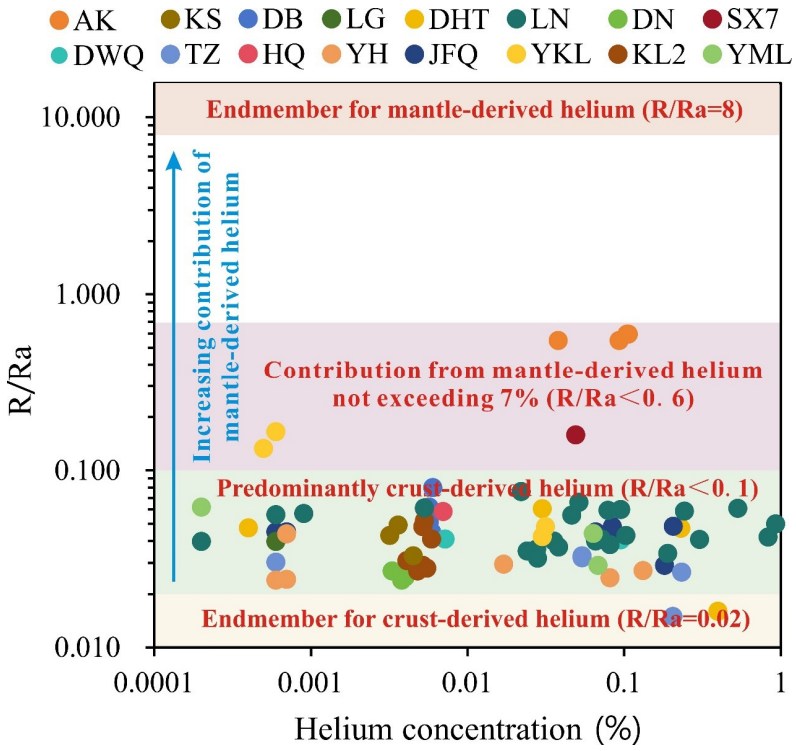

Figure 6. Characteristics of helium isotope for different oil and gas fields in the Tarim Basin. With the exception of the AK gas field that has an amount not exceeding 7% of mantle helium, all oil and gas fields include predominantly crust-derived helium.

5. Discussion

5.1. Abundant Helium Flux

Although both helium-4 and natural gases accumulate together in a trap, helium has remarkable intrinsic differences in genetic mechanism [51]. Unlike natural gas, helium-4 has an extremely slow production rate, which depends on both the very long half-life of U and Th elements (up to billions of years) and the low abundance of radioactive elements in helium-generating raw materials (helium source rocks), such as granite. Its accumulation in a trap, therefore, requires both long radioactive time and massive volume of helium source rocks.

Petroleum exploration campaigns have drilled the sedimentary records from the Sinian to the Quaternary in the Tarim Basin. These sedimentary strata overlay the Proterozoic basement granite-metamorphic rock mass. According to field observations and drilling activities, there are multiple basement magmatic and metamorphic rocks in the Tarim Basin. For example, the Ailiankate Rock Group in the Tielelike tectonic belt in the southern margin of this basin is mainly composed of epimetamorphic intermediate-acidic volcanic rocks and clastic rocks. U-Pb dating of zircon results show that this group is a Neoproterozoic succession deposited at ca. 780~800 Ma [52]. Also, the Haoluositan Rock Group in the same tectonic belt consists of magmatic granitic gneiss and hypersthene granulite, and U-Pb dating of the zircon determines that this group is a Mesoarchean succession deposited at ca. 3137.3 ± 4.1 Ma [53]. Well Tacan 1 that located in the central region of this basin drilled into the granodiorite beneath Cambrian strata at 7169~7200 m [54]. Well Shan53 and Well Qiaogu2 in the northwest region of this basin drilled into the Pre-Sinian granite with the age of 1.8 Ga [40].

These ancient and massive volumes of basement rock can provide abundant helium flux for the formation of helium-rich gas fields. In addition, hydrocarbon source rock is significantly enriched in U and Th compared to granite, up to the level of dozens of ppm level. Despite this, it cannot produce enough helium flux to form helium-rich gas fields due to the dilution of large amounts of gaseous hydrocarbons, even in the case

that a portion of gaseous hydrocarbons are discharged from source rock due to the effect of "hydrocarbon-generating pressurization". However, helium flux produced by only U-Th-rich hydrocarbon source rocks cannot be completely ignored. Though relatively rare, there is a natural example of a case favoring this valuable helium flux, the Wufeng-Longmaxi shale that widely developed in the Sichuan Basin, China [55–58]. According to the latest data, all Wufeng-Longmaxi commercial shale gas in service fields have helium concentrations between 0.02% and 0.05%, except that of the Pengshui gas field, which has helium concentrations between 0.08% and 0.1% [27]. Previous works documented that Cambrian Yuertusi Formation hydrocarbon source rocks with great thickness developed widely in the Traim Basin, particularly in the Tabei Uplift and Tazhong Depression, have very high U concentration, ranging from dozens to several hundreds of ppm [59–61]. It can be reasonably induced that this set of source rocks should provide valuable helium flux for local overlying helium-rich gas fields, although this contribution has been very difficult to quantitatively ascertain to date.

The presence or absence of helium source rocks as well as their abundance can be characterized quantitatively by using the responses of paleomagnetic anomalies. In the maps of aeromagnetic isogram in the Tarim Basin (Figure 7), oil and gas fields with helium concentrations above 0.05% all fall within the zones with strong magnetic induction intensity. However, not all zones with strong magnetic induction intensity overlap well with those fields with helium concentrations above economical threshold. This demonstrates that abundant helium flux is only a necessary condition, and not a sufficient condition for the existence of helium-rich gas fields.

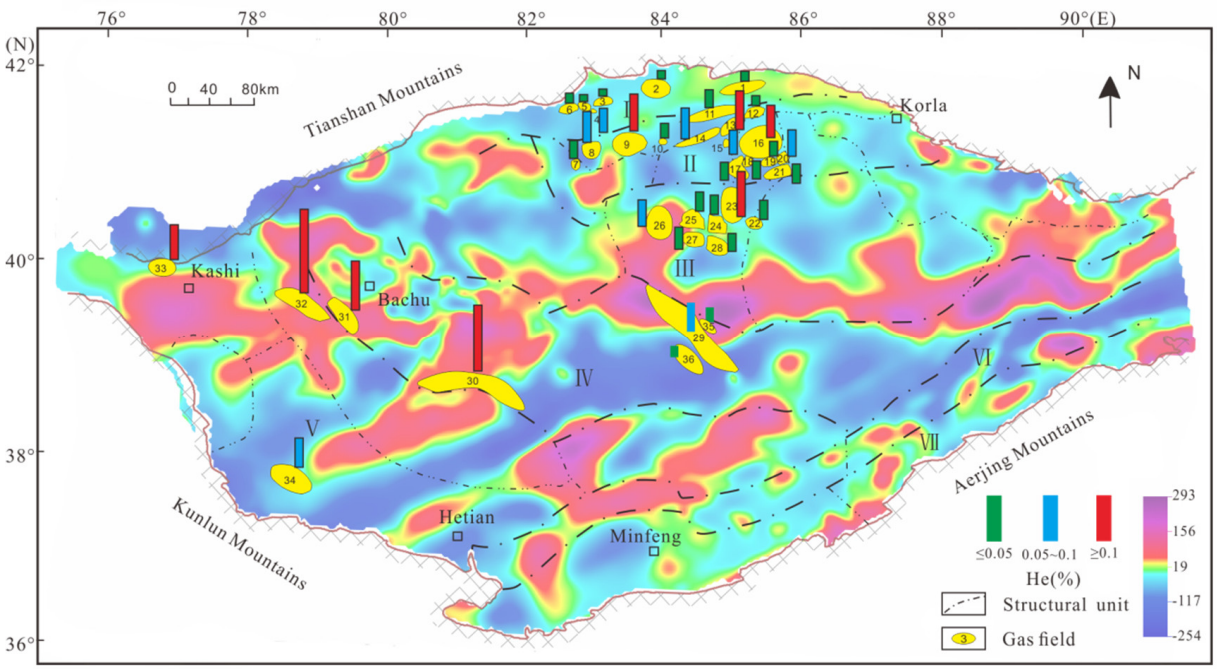

Figure 7. Maps of aeromagnetic display in the Tarim Basin as well as helium concentrations for 36 oil and gas fields. These zones displaying strong magnetism indicate intensive helium-generated capacity. In the Southwest Depression, helium-rich gas fields (He > 0.1%) are consistent with strong magnetism. Helium-rich gas fields mainly located in the Tabei Uplift are related to local igneous intrusion, such as the YML oil and gas fields and HD oil fields. I: Kuqa Depression, II: Tabei Uplift, III: North Depression, IV: Central Uplift, V: Southwest Depression, VI: Southeast Uplift, VII: Southeast Depression. 1: DN, 2: KL2, 3: KS, 4: DWQ, 5: DB, 6: BZ, 7: YD, 8: YTK, 9: YML, 10: HQQ, 11: YH, 12: DLB, 13: YKL, 14: DHT, 15: QG, 16: LN, 17: TH, 18: LG, 19: STM, 20: JFQ, 21: JLK, 22: YK, 23: HD, 24: FY, 25: YM, 26: SB, 27: GL, 28: MS, 29: TZ, 30: HTH, 31: YSD, 32: BSTP, 33: AK, 34: KKY, 35: ZH, 36: ZG.

5.2. Presence of Developed Faults between the Source and Reservoir Systems

As discussed earlier, helium in oil and gas fields in the Tarim Basin considerably originates from the basement rocks. These helium flows migrating upward into the reservoirs require deep-rooted faults that connect the source and reservoir systems. This seems to be confirmed because high helium concentrations are always localized near faults. These deep-rooted faults are the byproducts of tectonic processes during the formation of geological faults and folds [62–65].

Unlike gaseous hydrocarbons, helium cannot form a continuous fluid alone due to its extremely low production rate. Some carriers or accompanying components are required before helium enters a trap or reservoir. The accompanying components vary greatly and include non-hydrocarbon gases (i.e., N_2, CO_2), formation water, and hydrocarbon fluids (including liquid and gaseous), which are closely related to the flux of accompanying components, as well as the formation and evolution of faults due to tectonic activities. Generally, before encountering hydrocarbon fluids, accompanying components are either formation water or N_2, which depends on whether N_2 in formation water reaches saturation [66]. After encountering hydrocarbon fluids, they migrate together into a trap or reservoir.

The HTH gas field located in the Mazhatage tectonic belt in the southern margin of the Bachu Uplift is the first supergiant helium-rich field discovered in the Tarim Basin. This gas field has two sets of reservoirs, Permian clastic limestone and Ordovician buried hill, both including helium concentration above 0.3% [5]. Due to multiple tectonic movements, some deep-rooted faults with different scales extend downward to the basement and are available for the migration of helium flow into overlying reservoirs (Figure 8).

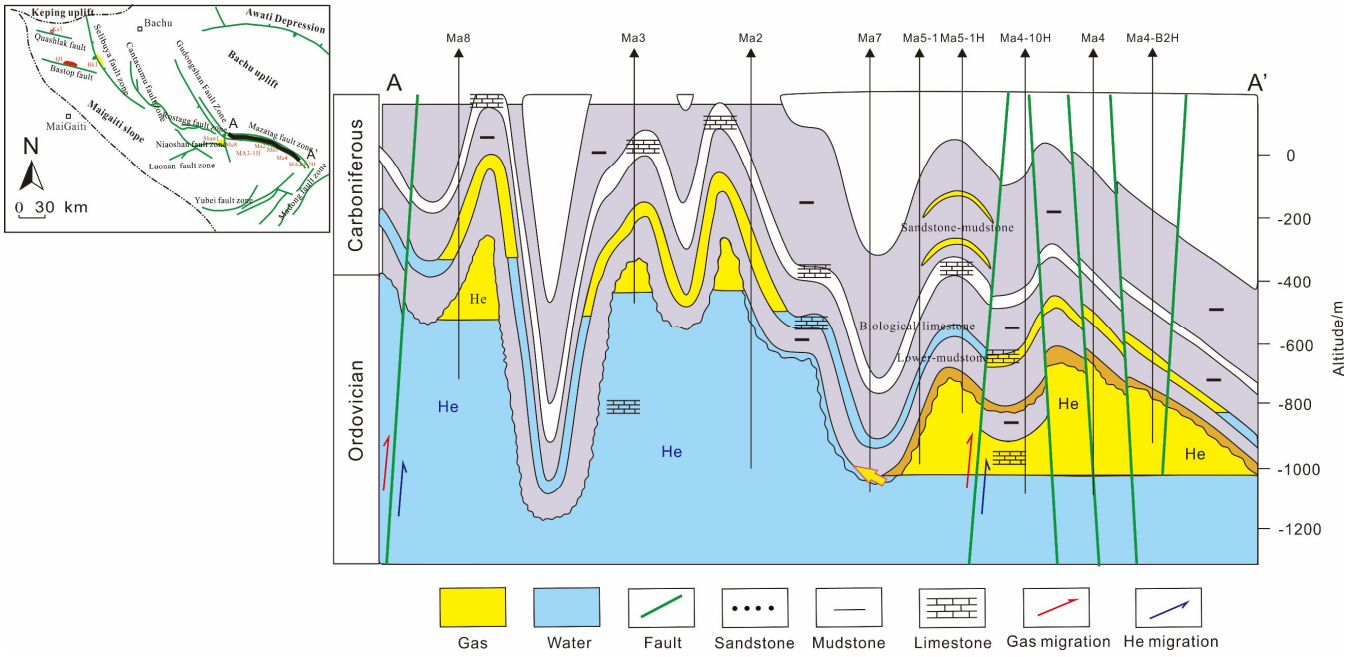

Figure 8. Top left: Map of Hetianhe gas field and its peripheral tectonic characteristics, as well as the A—A′ location. Right: A—A′ cross section, showing the major gas-bearing stratigraphic sequences and deep-seated faults.

The YKL gas field that is located in the middle section of the Yakela fault-convex in the Shaya Uplift has multiple intervals of commercial reservoirs, such as Cambrian, Ordovician, Cretaceous, and Paleogene. These intervals all contain helium, but the concentrations differ greatly. Specifically, many samples from the Cambrian and Ordovician reservoirs have helium concentrations between 0.03% and 0.94%, while those from the Cretaceous reservoir are between 0.04% and 0.19%, and those from the Paleogene reservoir are far below 0.1% [13,14,34,35,40]. Such distributions of helium concentrations in this gas field are

attributed to the presence of two deep-seated faults, the Luntai fault to the north and the Yanan fault to the south. These two faults both extend downward into the Paleozoic strata and Proterozoic basement, favoring the upward migration of helium flow. However, these two faults both do not penetrate through Cretaceous strata (Figure 9). In addition, there are two sets of caprocks (Jurassic coal-bearing mudstones and Paleogene Suweiyi Formation gypsum mudstones), preventing the emission of helium from both gas reservoirs. In these cases, the Paleogene reservoir has very low helium concentrations due to lack of the helium flow from the ancient basement.

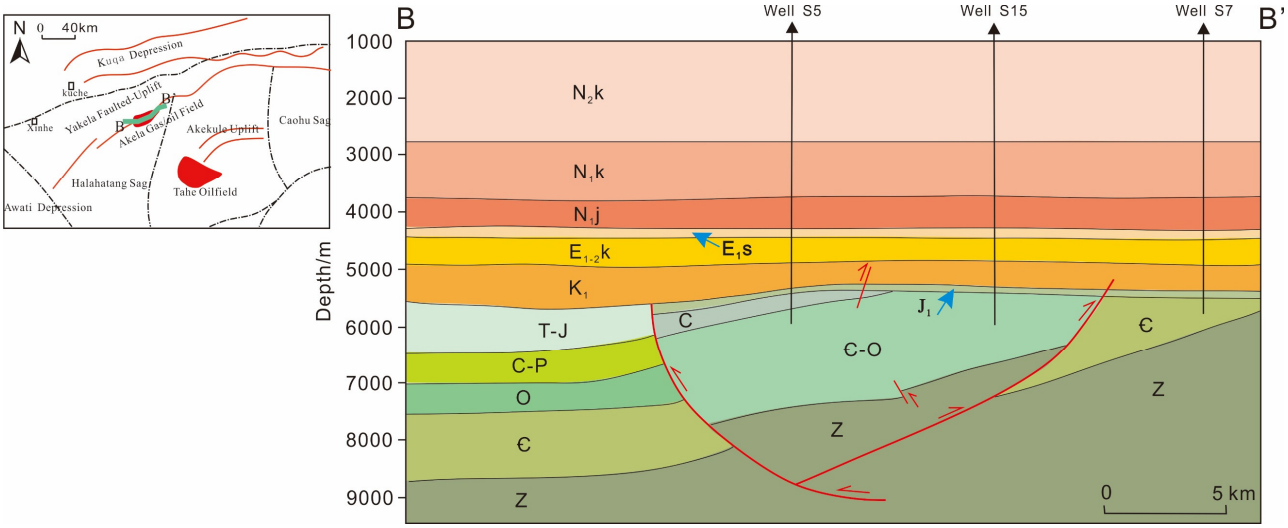

Figure 9. Top left: Map of Yakela gas field and its peripheral tectonic characteristics, as well as the B−B′ location. Right: B−B′ cross section, showing the major stratigraphic sequences and deep-seated faults.

5.3. Intensity of Hydrocarbon Generation Versus Helium Concentarion

The diffusion coefficient is a commonly used proxy to represent diffusion capacity of certain fluids [67,68]. Helium in the Tarim Basin is mainly associated with gaseous hydrocarbons, mainly CH_4 in the oil and gas fields. Only considering the thermal diffusion behavior and without the constraint from caprock, helium diffusion is significantly smaller in the helium-CH_4 mixing system than in the solely helium system; moreover, it tends to reduce with the decrease in helium concentration for the helium-CH_4 mixing system [51]. Following the theoretical calculation results, it can be reasonably inferred that the presence of CH_4 in a helium-rich gas field, as a carrier for helium occurrence at a geological timescale, causes the decrease in helium emission loss via diffusion. This may explain why, to date, no pure helium or high-grade helium field has been discovered in nature.

From the perspective of the grade of helium, which is a key parameter that must be considered for helium extraction technology, the existence of a great deal of CH_4 is evidently very unfavorable. Indeed, we observed that there is a negative correlation between helium concentration and hydrocarbon-generating intensity of the Lower Jurassic hydrocarbon source rocks in the Kuqa Depression (Figure 10). This is attributed to the strong dilution of gaseous hydrocarbons. For this reason, exploration campaigns specifically targeting helium resources should avoid the sedimentation depocenter of hydrocarbon source rocks. On the contrary, more attention should be paid to slope belts and tectonically high positions (i.e., uplift zones in the cratonic basin).

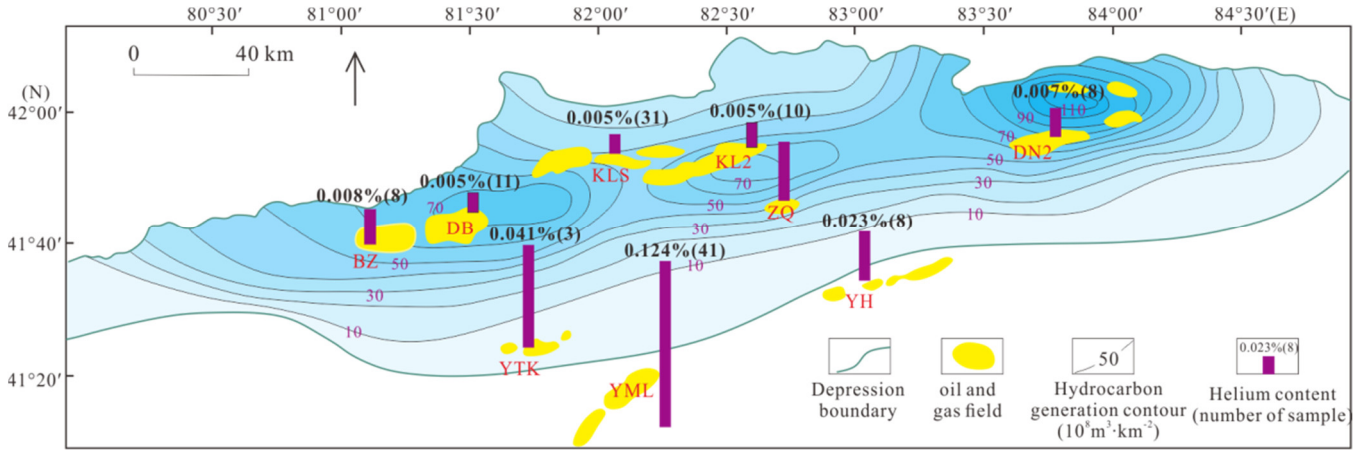

Figure 10. Relationships between helium concentrations and hydrocarbon-generating intensity for the main gas fields of the Kuqa Depression. Overall, with the increase in hydrocarbon-generating intensity, the helium concentrations of gas fields gradually decrease.

5.4. Presence of Dense Caprock

Helium has stronger diffusion than gaseous hydrocarbons, and the sealing capacity of caprock is vital for the preservation of helium-rich gas fields at a geological timescale. Li et al. [51] summarized the caprock types of typical helium-rich gas fields around the globe, finding that those gas fields in the USA with high helium concentrations, such as Hugoton-Panhandle (0.53%), Cliffside (1.8%), Doe Canyon (5.01%), and Big Piney-La Barge (0.5%), all have either gypsum, evaporite, or salt rocks as caprocks. By contrast, these helium-rich gas fields discovered in China have thick mudstones as caprock, thus resulting in relatively lower helium concentrations, such as 0.13% for the Dongsheng gas field [7] and 0.26% for Weiyuan gas field [69]. To sum up, similar to natural gas, dense gypsum, evaporite, and salt rocks have superior sealing capacity to mudstones for helium.

In the present study, we collected the caprock characteristics of oil and gas fields in the Tarim Basin that have average helium concentrations above 0.1%, as shown in Table 1. These helium-rich oil and gas fields, such as the HTH, AK, YKL, and HD Zone-4, have the caprock of mostly gypsum-bearing mudstones.

Table 1. Caprock characteristics of helium-rich oil and gas fields in the Tarim Basin.

Helium-Rich Gas Fields	Helium Concentration (%)	Caprock
HTH	0.27~0.42%	Carboniferous mudstone and gypsum-bearing mudstone of Bachu Formation and Kalashai Formation
AK	0.10~0.12%	Paleogene gypsum-bearing mudstone
HD Zone-4	Below 0.01~0.69%	Carboniferous gypsum-bearing mudstone of Bachu Formation
TZ Zone-4	Far below 0.01~0.55%	Carboniferous thick mudstone
YKL	Far below 0.01~2.19%	Carboniferous gypsum-bearing mudstone of Bachu Formation
BS	0.11~0.73%	Permian mudstone of Nanzha Formation
YSD	0.22%	Permian mudstone of Nanzha Formation
YML	Far below 0.01~0.34%	Cretaceous gypsum-bearing mudstone of Kapusaliang Formation
LN	Far below 0.01~0.93%	Triassic gypsum-bearing mudstone of Huangshanjie Formation

5.5. Favorable Zones for Helium Exploration in the Tarim Basin

Helium exploration is primarily based on the following three basic principles: (1) helium concentration in the oil and gas fields is vital because it is associated with the selection of extraction technology; (2) evaluation on the reserve scale of natural gas for matured oil and gas production zones need to be considered, and it is closely related to facility location and scale; (3) helium grade must be considered for oil and gas exploration or prospective zones.

Diverse grades of helium concentrations exist in different secondary tectonic units in the Tarim Basin. Moreover, oil and gas phase states in these units also vary greatly. In the Kuqa Depression, the reserves of natural gas fields are exceedingly abundant, whereas helium concentrations in these gas fields are far below economical threshold. Although helium reserves, helium concentrations multiplied by the reserves of natural gas, are quite good, this tectonic unit is inadequate for helium extraction due to the extremely low helium concentration. In the Tabei Uplift, some fields have both considerable reserves of natural gas and high helium concentrations, such as LN, YKL, and YML. Although some oil and gas fields in the North Depression and Tazhong Uplift have considerable helium concentrations, such as HD Zone-4, TZ Zone-4, and certain fault zones in the SB oil and gas fields, their reserves of associated natural gas, as well as daily production, are limited. These oil and gas fields are, therefore, not favorable zones for large-scale helium extraction. Most of gas fields discovered in the Southwest Depression include high helium concentrations, such as the HTH and AK gas fields. In recent years, natural gas exploration campaigns targeting the Mesozoic strata have made significant breakthroughs, and the typical wells, such as well Qiatan-1, Abei-1, and Luosi-2, show fairly good gas flow, indicative of the enormous potential for natural gas exploration in the southwestern Tarim Basin piedmont [70]. Moreover, these new wells include helium concentrations close to or above 0.1% [5,70]. Therefore, this secondary tectonic unit is the most favorable zone for future helium extraction.

6. Conclusions

(1) According to helium isotope characteristics, except for the AK gas field, which has a mantle helium not exceeding 7%, all oil and gas fields in the Tarim Basin are predominantly crust-derived helium.

(2) Helium concentrations vary greatly across different oil and gas fields. Helium-rich gas fields (He > 0.1%) are mainly concentrated in the Tabei Uplift and Southwest Depression in the Tarim Basin. Moreover, there are considerably abundant natural gas reserves in these two tectonic units. Therefore, these helium-rich oil and gas fields in these two tectonic units are favorable zones of further deployment for helium extraction in the Tarim Basin.

(3) The formation of helium-rich system is controlled by multiple factors. Helium accumulation requires abundant helium flux. Developed fault systems are effective migration pathways for helium-rich fluids. Strong hydrocarbon-generating intensity causes the decrease in helium concentrations for gas fields due to intensive dilution. Thick mudstone and gypsum-bearing mudstone favor helium preservation over a geological timescale.

Supplementary Materials: The following supporting information can be downloaded at https://www.mdpi.com/article/10.3390/pr12071469/s1. Table S1: Characteristics of helium concentrations for 36 oil and gas fields in the Tarim Basin. References cited in the supplementary file [10,13,14,30–40].

Author Contributions: Conceptualization, H.Y., P.L., H.Z. and W.Z.; methodology, H.Y., H.Z. and W.Z.; formal analysis, H.Y., P.L., H.Z., J.L. (Jiahao Lv), W.Z., J.L. (Jiarun Liu), S.H., X.Y., W.Y. and X.W.; investigation, H.Y., P.L. and H.Z.; data curation, P.L., J.L. (Jiahao Lv) and J.L. (Jiarun Liu); writing—original draft, H.Y., P.L., H.Z., J.L. (Jiahao Lv), W.Z., J.L. (Jiarun Liu) and S.H.; writing—review & editing, H.Y., P.L. and H.Z.; visualization, P.L., J.L. (Jiahao Lv) and J.L. (Jiarun Liu); project administration, H.Y., P.L., H.Z. and W.Z.; funding acquisition, H.Y. and P.L. All authors have read and agreed to the published version of the manuscript.

Funding: This work was supported by the National Natural Science Foundation of China (Grant Nos. 42203027 and U2244209), China Postdoctoral Science Foundation (Grant No. 2023M730039), and Scientific research and technology development project of China National Petroleum Corporation Limited (Grant No. 2021ZG13).

Data Availability Statement: The data presented in this study are available on request from the corresponding author.

Conflicts of Interest: Authors Haijun Yang, Haizu Zhang, Wen Zhang, Shaoying Huang, Xianzhang Yang, Wenfang Yuan and Xiang Wang were employed by the China National Petroleum Corporation (CNPC). Author Wen Zhang was employed by the Tarim Oilfield Company. The remaining authors declare that the research was conducted in the absence of any commercial or financial relationships that could be construed as a potential conflict of interest. The China National Petroleum Corporation (CNPC) and Tarim Oilfield Company had no role in the design of the study; in the collection, analyses, or interpretation of data; in the writing of the manuscript, or in the decision to publish the results.

Abbreviations

Dina: DN, Kela2: KL2, Keshen: KS, Dawanqi: DWQ, Dabei: DB, Bozi: BZ, Yudong, YD, Yangtake: YTK, Yingmaili: YML, Hongqiqu: HQQ, Yaha: YH, Dalaoba: DLB, Yakela: YKL, Donghetang: DHT, Qiangu: QG, Lunnan: LN, Tahe: TH, Lungu: LG, Sangtamu: STM, Jiefangqu: JFQ, Jilake: JLK, Yuke: YK, Hade: HD, Fuyuan: FY, Yueman: YM, Shunbei: SB, Guole: GL, Manshen: MS, Tazhong: TZ, Hetianhe: HTH, Yasongdi: YSD, Bashituopu: BSTP, Akemomu: AK, Kekeya: KKY, Zhonghan: ZH, Zhonggu: ZG.

References

1. Glowacki, B.A.; Nuttall, W.J.; Clarke, R.H. Beyond the Helium Conundrum. *IEEE Trans. Appl. Supercond.* **2013**, *23*, 0500113. [CrossRef]
2. Nuttall, W.J.; Clarke, R.H.; Glowacki, B.A. Stop squandering helium. *Nature* **2012**, *485*, 573–575. [CrossRef] [PubMed]
3. Siddhantakar, A.; Santillán-Saldivar, J.; Kippes, T.; Sonnemann, G.; Reller, A.; Young, S.B. Helium resource global supply and demand: Geopolitical supply risk analysis. *Resour. Conserv. Recycl.* **2023**, *193*, 106935. [CrossRef]
4. USGS. *Helium Statistics and Information*; United States Geologic Survey National Minerals Information Centre: Reston, VA, USA, 2024.
5. Tao, X.; Li, J.; Zhao, L.; Li, L.; Zhu, W.; Xing, L.; Su, F.; Shan, X.; Zheng, H.; Zhang, L. Helium resources and discovery of first supergiant helium reserve in China: Hatianhe gas field. *Earth Sci.* **2019**, *44*, 1024–1041.
6. Liu, Q.; Wu, X.; Jia, H.; Ni, C.; Zhu, J.; Miao, J.; Zhu, D.; Meng, Q.; Peng, W.; Xu, H. Geochemical Characteristics of Helium in Natural Gas From the Daniudi Gas Field, Ordos Basin, Central China. *Front. Earth Sci.* **2022**, *10*, 823308. [CrossRef]
7. Peng, W.; Liu, Q.; Zhang, Y.; Jia, H.; Zhu, D.; Meng, Q.; Wu, X.; Deng, S.; Ma, Y. The first extra-large helium-rich gas field identified in a tight sandstone of the Dongsheng Gas Field, Ordos Basin, China. *Sci. China Earth Sci.* **2022**, *65*, 874–881. [CrossRef]
8. Liu, Q.; Li, P.; Zhu, D.; Zhu, D.; Wu, X.; Wang, X.; Tao, X.; Meng, Q.; Xu, H.; Gao, Y.; et al. Helium resource in the petroliferous basins in China and its development prospects. *Cell Rep. Phys. Sci.* **2024**, *5*, 102031. [CrossRef]
9. Danabalan, D. Helium: Exploration Methodology for a Strategic Resource. Ph.D. Thesis, Durham University, Durham, UK, 2017.
10. Dai, J.; Gong, D.; Ni, Y.; Huang, S.; Wu, W. Stable carbon isotopes of coal-derived gases sourced from the Mesozoic coal measures in China. *Org. Geochem.* **2014**, *74*, 123–142. [CrossRef]
11. Dai, J.; Qin, S.; Hu, G.; Ni, Y.; Gan, L.; Huang, S.; Hong, F. Major progress in the natural gas exploration and development in the past seven decades in China. *Pet. Explor. Dev.* **2019**, *46*, 1100–1110. [CrossRef]
12. Dai, J.; Zou, C.; Li, J.; Ni, Y.; Hu, G.; Zhang, X.; Liu, Q.; Yang, C.; Hu, A. Carbon isotopes of Middle–Lower Jurassic coal-derived alkane gases from the major basins of northwestern China. *Int. J. Coal Geol.* **2009**, *80*, 124–134. [CrossRef]
13. Liu, Q.; Jin, Z.; Li, H.; Wu, X.; Tao, X.; Zhu, D.; Meng, Q. Geochemistry characteristics and genetic types of natural gas in central part of the Tarim Basin, NW China. *Mar. Pet. Geol.* **2018**, *89*, 91–105. [CrossRef]
14. Liu, Q.; Zhijun, J.; Jianfa, C.; Krooss, B.M.; Qin, S. Origin of nitrogen molecules in natural gas and implications for the high risk of N_2 exploration in Tarim Basin, NW China. *J. Pet. Sci. Eng.* **2012**, *81*, 112–121. [CrossRef]
15. Peng, W.; Lin, H.; Liu, Q.; Deng, S.; Zhang, J.; Zhang, Y.; Feng, F.; Ma, A.; Zhou, B. Geochemical characteristics of helium and favorable exploration areas in the Tarim Basin, China. *Nat. Gas Geosci.* **2023**, *34*, 576–586.
16. Danabalan, D.; Gluyas, J.G.; Macpherson, C.G.; Abraham-James, T.H.; Bluett, J.J.; Barry, P.H.; Ballentine, C.J. The principles of helium exploration. *Pet. Geosci.* **2022**, *28*, petgeo2021-029. [CrossRef]
17. Cui, Y.; Sun, F.; Liu, L.; Xie, C.; Li, J.; Chen, Z.; Li, Y.; Du, J. Contribution of deep-earth fluids to the geothermal system: A case study in the Arxan volcanic region, northeastern China. *Front. Earth Sci.* **2023**, *10*, 996583. [CrossRef]
18. Halford, D.T.; Karolytė, R.; Barry, P.H.; Whyte, C.J.; Darrah, T.H.; Cuzella, J.J.; Sonnenberg, S.A.; Ballentine, C.J. High helium reservoirs in the Four Corners area of the Colorado Plateau, USA. *Chem. Geol.* **2022**, *596*, 120790. [CrossRef]

19. Zhang, W.; Li, Y.; Zhao, F.; Han, W.; Li, Y.; Wang, Y.; Holland, G.; Zhou, Z. Using noble gases to trace groundwater evolution and assess helium accumulation in Weihe Basin, central China. *Geochim. Cosmochim. Acta* **2019**, *251*, 229–246. [CrossRef]
20. Klemperer, S.L.; Zhao, P.; Whyte, C.J.; Darrah, T.H.; Crossey, L.J.; Karlstrom, K.E.; Liu, T.; Winn, C.; Hilton, D.R.; Ding, L. Limited underthrusting of India below Tibet: $^{3}He/^{4}He$ analysis of thermal springs locates the mantle suture in continental collision. *Proc. Natl. Acad. Sci. USA* **2022**, *119*, e2113877119. [CrossRef]
21. Hiett, C.D.; Newell, D.L.; Jessup, M.J.; Grambling, T.A.; Scott, B.E.; Upin, H.E. Deep CO_2 and N_2 emissions from Peruvian hot springs: Stable isotopic constraints on volatile cycling in a flat-slab subduction zone. *Chem. Geol.* **2022**, *595*, 120787. [CrossRef]
22. Dai, J.; Ni, Y.; Qin, S.; Huang, S.; Gong, D.; Liu, D.; Feng, Z.; Peng, W.; Han, W.; Fang, C. Geochemical characteristics of He and CO 2 from the Ordos (cratonic) and Bohaibay (rift) basins in China. *Chem. Geol.* **2017**, *469*, 192–213. [CrossRef]
23. Qin, S.; Li, J.; Liang, C.; Zhou, G.; Yuan, M. Helium enrichment model of helium-rich gas reservoirs in petroliferous basins in China. *Nat. Gas Ind.* **2022**, *42*, 125–134. [CrossRef]
24. Liu, Q.; Dai, J.; Jin, Z.; Li, J.; Wu, X.; Meng, Q.; Yang, C.; Zhou, Q.; Feng, Z.; Zhu, D. Abnormal carbon and hydrogen isotopes of alkane gases from the Qingshen gas field, Songliao Basin, China, suggesting abiogenic alkanes? *J. Asian Earth Sci.* **2016**, *115*, 285–297. [CrossRef]
25. Ni, Y.; Dai, J.; Tao, S.; Wu, X.; Liao, F.; Wu, W.; Zhang, D. Helium signatures of gases from the Sichuan Basin, China. *Org. Geochem.* **2014**, *74*, 33–43. [CrossRef]
26. Wang, X.; Liu, Q.; Liu, W.; Zhang, D.; Li, X.; Zhao, D. Accumulation mechanism of mantle-derived helium resources in petroliferous basins, eastern China. *Sci. China Earth Sci.* **2022**, *65*, 2322–2334. [CrossRef]
27. Nie, H.; Liu, Q.; Dang, W.; Li, P.; Su, H.; Bao, H.; Xiong, L.; Liu, Z.; Sun, C.; Zhang, P. Enrichment mechanism and resource potential of shale-type helium: A case study of Wufeng Formation-Longmaxi Formation in Sichuan Basin. *Sci. China Earth Sci.* **2023**, *66*, 1279–1288. [CrossRef]
28. Wang, Q.; Xu, Z.; Zhang, R.; Yang, H.; Yang, X. New fields, new types of hydrocarbon explorations and their resource potentials in Tarim Basin. *Acta Pet. Sin.* **2024**, *45*, 15–32.
29. Liu, Q.; Jin, Z.; Zhang, D.; Liu, Z.; Li, J. Geochemical Characteristics and Genesis of Natural Gas in Tarim Basin. *Nat. Gas Geosci.* **2008**, *19*, 234–237.
30. Xu, Y.; Shen, P.; Liu, W.; Tao, M.; Sun, M.; Du, J. *Noble Gas Geochemistry in Natural Gas*; Science Press: Beijing, China, 1998.
31. Chen, J.; Xu, Y.; Huang, D. Geochemical Characteristics and Origin of Natural Gas in Tarim Basin, China. *AAPG Bull.* **2000**, *84*, 591–606.
32. Qin, S.; Li, X.; Xiao, Z.; Li, M.; Zhang, Q. Geochemistry, origin and distribution of natural gases in Tarim Basin, NW China. *Pet. Explor. Dev.* **2005**, *32*, 70–78.
33. Liu, Q.; Dai, J.; Jin, Z.; Li, J. Geochemistry and Genesis of Natural Gas in the Foreland and Platform of the Tarim Basin. *Acta Geol. Sin.* **2009**, *83*, 107–114.
34. Yu, Q.; Shi, Z.; Wang, D.; Guo, H. Analysis on helium enrichment characteristics and reservoir forming conditions in Northwest Tarim Basin. *Northwestern Geol.* **2013**, *46*, 215–222.
35. He, D.; Chen, J.; Zhang, C.; Li, W.; Zhou, J. Compositions of non-hydrocarbon and noble gases in natural gas samples from Tarim Basin, China. *Geochem. J.* **2015**, *49*, 271–282. [CrossRef]
36. Wang, X.; Chen, J.; Li, Z.; Li, J.; Wang, D.; Wang, Y.; Yang, C.; Cui, H. Rare gases geochemical characteristics and gas source correlation for Dabei gas field in Kuche depression, Tarim Basin. *Energy Explor. Exploit.* **2016**, *34*, 113–128. [CrossRef]
37. Wang, X.; Wei, G.; Li, J.; Chen, J.; Gong, S.; Li, Z.; Wang, D.; Xie, Z.; Yang, C.; Wang, Y.; et al. Geochemical characteristics and origins of noble gases of the Kela 2 gas field in the Tarim Basin, China. *Mar. Pet. Geol.* **2018**, *89*, 155–163. [CrossRef]
38. Wang, X.; Zou, C.; Li, J.; Wei, G.; Chen, J.; Xie, Z.; Li, Z.; Guo, J.; Lin, S.; Pan, S.; et al. Comparison on Rare Gas Geochemical Characteristics and Gas Originations of Kuche and Southwestern Depressions in Tarim Basin, China. *Geofluids* **2019**, *2019*, 1786–1802. [CrossRef]
39. He, D.; Tang, Y.; Hu, J.; Mo, S.; Chen, J. Geochemical characteristics of noble gases in natural gases from the Tarim Basin. *Oil Gas Geol.* **2020**, *41*, 755–762.
40. Han, Q.; Geng, F.; Hu, B.; Gao, S.; Jin, X.; Wang, X.; Li, Z. Investigation and study on helium gas reservoir resources in Sinopec exploration area of Tarim Basin. *J. Palaeogeogr.* **2022**, *24*, 1029–1036.
41. Li, Y.; Sun, L.; Yang, H.; Zhang, G.; Zeng, C.; Feng, X.; Wen, L.; Zhang, Q.; Jia, T. New discovery of Late Silurian-Carboniferous extensional structure in Tarim Basin and its geological significance. *Chin. J. Geol.* **2014**, *49*, 30–48. [CrossRef]
42. Tian, W.; Campbell, I.H.; Allen, C.M.; Guan, P.; Pan, W.; Chen, M.; Yu, H.; Zhu, W. The Tarim picrite–basalt–rhyolite suite, a Permian flood basalt from northwest China with contrasting rhyolites produced by fractional crystallization and anatexis. *Contrib. Mineral. Petrol.* **2010**, *160*, 407–425. [CrossRef]
43. Liu, Q.; Wu, X.; Wang, X.; Jin, Z.; Zhu, D.; Meng, Q.; Huang, S.; Liu, J.; Fu, Q. Carbon and hydrogen isotopes of methane, ethane, and propane: A review of genetic identification of natural gas. *Earth-Sci. Rev.* **2019**, *190*, 247–272. [CrossRef]
44. Wakita, H.; Sano, Y. $^{3}He/^{4}He$ ratios in CH_4-rich natural gases suggest magmatic origin. *Nature* **1983**, *305*, 792–794. [CrossRef]
45. Polyak, B.G.; Tolstikhin, I.N. Isotopic composition of the earth's helium and the problem of the motive forces of tectogenesis. *Chem. Geol.* **1985**, *52*, 9–33. [CrossRef]
46. Oxburgh, E.R.; O'Nions, R.K.; Hill, R.I. Helium isotopes in sedimentary basin. *Nature* **1986**, *324*, 632–635. [CrossRef]

47. Xu, S.; Nakai, S.I.; Wakita, H.; Xu, Y.; Wang, X. Helium isotope compositions in sedimentary basins in China. *Appl. Geochem.* **1995**, *10*, 634–656. [CrossRef]
48. Craig, H.; Lupton, J.E. Primordial neon, helium and hydrogen in oceanic basalts. *Earth Planet. Sci. Lett.* **1976**, *31*, 369–385. [CrossRef]
49. Kurz, M.D.; Jenkins, W.J. The distribution of helium in oceanic basalt glasses. *Earth Planet. Sci. Lett.* **1981**, *53*, 41–54. [CrossRef]
50. Poreda, R.; Schilling, J.-G.; Craig, H. Helium and hydrogen isotopes in ocean-ridge basalts north and south of Iceland. *Earth Planet. Sci. Lett.* **1986**, *78*, 1–17. [CrossRef]
51. Li, P.; Liu, Q.; Zhu, D.; Zhu, D.; Zhou, Z.; Wu, X.; Meng, Q.; Lv, J.; Gao, Y. Distributions and accumulation mechanism of helium in petroliferous basins. *Sci. China Earth Sci.* **2024**. [CrossRef]
52. Wang, C.; Liu, L.; Che, Z.; He, S.; Li, R.; Yang, W.; Cao, Y.; Zhu, X. Zircon U-Pb and Hf isotope from the east segment of Tiekelike tectonic belt: Constrains on the timing of Precambrian basement at the southwestern margin of Tarim, China. *Acta Geol. Sin.* **2009**, *83*, 1646–1655.
53. Guo, X.; Zheng, Y.; Gao, J.; Zhu, Z. Determination and geological significance of the Mesoarchean craton in Western Kunlun Mountains, Xinjiang, China. *Geol. Rev.* **2013**, *59*, 401–412.
54. Li, Y.; Song, W.; Wu, G.; Wang, Y.; Li, Y.; Zheng, D. Jinning granodiorite and diorite deeply concealed in the central Tarim Basin. *Sci. China Ser. D Earth Sci.* **2005**, *48*, 2061–2068. [CrossRef]
55. Zou, C.; Dong, D.; Wang, Y.; Li, X.; Huang, J.; Wang, S.; Guan, Q.; Zhang, C.; Wang, H.; Liu, H.; et al. Shale gas in China: Characteristics, challenges and prospects (I). *Pet. Explor. Dev.* **2015**, *42*, 753–767. [CrossRef]
56. Dai, J.; Zou, C.; Dong, D.; Ni, Y.; Wu, W.; Gong, D.; Wang, Y.; Huang, S.; Huang, J.; Fang, C.; et al. Geochemical characteristics of marine and terrestrial shale gas in China. *Mar. Pet. Geol.* **2016**, *76*, 444–463. [CrossRef]
57. Zou, C.; Zhu, R.; Chen, Z.-Q.; Ogg, J.G.; Wu, S.; Dong, D.; Qiu, Z.; Wang, Y.; Wang, L.; Lin, S.; et al. Organic-matter-rich shales of China. *Earth-Sci. Rev.* **2019**, *189*, 51–78. [CrossRef]
58. Zou, C.; Qiu, Z.; Zhang, J.; Li, Z.; Wei, H.; Liu, B.; Zhao, J.; Yang, T.; Zhu, S.; Tao, H.; et al. Unconventional Petroleum Sedimentology: A Key to Understanding Unconventional Hydrocarbon Accumulation. *Engineering* **2022**, *18*, 62–78. [CrossRef]
59. Zhu, G.; Li, T.; Zhao, K.; Li, C.; Cheng, M.; Chen, W.; Yan, H.; Zhang, Z.; Algeo, T.J. Mo isotope records from Lower Cambrian black shales, northwestern Tarim Basin (China): Implications for the early Cambrian ocean. *GSA Bull.* **2021**, *134*, 3–14. [CrossRef]
60. Gao, Z.; Shi, J.; Lv, J.; Chang, Z. High-frequency sequences, geochemical characteristics, formations, and distribution predictions of the lower Cambrian Yuertusi Formation in the Tarim Basin. *Mar. Pet. Geol.* **2022**, *146*, 105966. [CrossRef]
61. Li, T.; Zhang, Y.; Zhu, G.; Chen, Z.; Li, X. Environmental controls on organic matter enrichment of the lower Cambrian source rocks in the Tarim Basin, Northwest China. *Mar. Pet. Geol.* **2023**, *158*, 106539. [CrossRef]
62. Islamov, S.; Islamov, R.; Shelukhov, G.; Sharifov, A.; Sultanbekov, R.; Ismakov, R.; Agliullin, A.; Ganiev, R. Fluid-Loss Control Technology: From Laboratory to Well Field. *Processes* **2024**, *12*, 114. [CrossRef]
63. Zhang, Y.; He, D.; Wu, B.; Gao, H. Kinematic evolution of fold-and-thrust belts in the Yubei-Tangbei area: Implications for tectonic events in the southern Tarim Basin. *Geosci. Front.* **2021**, *12*, 101233. [CrossRef]
64. Chen, S.; Zhang, Y.; Xie, Z.; Song, X.; Liang, X. Multi-stages of Paleozoic deformation of the fault system in the Tazhong Uplift, Tarim Basin, NW China: Implications for hydrocarbon accumulation. *J. Asian Earth Sci.* **2024**, *265*, 106086. [CrossRef]
65. Zhong, Z.; Hou, G.; Xia, J.; Li, X.; Wei, L.; Chang, H. Detrital zircon U-Pb geochronology of Ordovician-Silurian strata in the northwestern platform of the Tarim Basin: Implications for provenance systems and tectonic evolution. *Gondwana Res.* **2024**, *134*, 1–20. [CrossRef]
66. Cheng, A.; Sherwood Lollar, B.; Gluyas, J.G.; Ballentine, C.J. Primary N_2–He gas field formation in intracratonic sedimentary basins. *Nature* **2023**, *615*, 94–99. [CrossRef]
67. Li, P.; Zhang, X.; Zhang, S. Response of methane diffusion in varying degrees of deformed coals to different solvent treatments. *Curr. Sci.* **2018**, *115*, 2155–2161. [CrossRef]
68. Sun, Z.; Li, P.; Zhou, S. A laboratory observation for gases transport in shale nanochannels: Helium, nitrogen, methane, and helium-methane mixture. *Chem. Eng. J.* **2023**, *472*, 144939. [CrossRef]
69. Liu, K.; Chen, J.; Fu, R.; Wang, H.; Luo, B.; Dai, X.; Yang, J. Discussion on distribution law and controlling factors of helium-rich natural gas in Weiyuan gas field. *J. China Univ. Pet.* **2022**, *46*, 12–21.
70. Wang, Q.; Yang, H.; Li, Y.; Cai, Z.; Yang, X.; Xu, Z.; Chen, C.; Sun, C. Major breakthrough in the Carboniferous-Permian in Well Qiatan 1 and exploration prospect in the piedmont southwestern Tarim Basin. *China Pet. Explor.* **2023**, *28*, 34–45.